Initial injury observations in postmortem human subjects: Non-penetrating ballistic impacts over the sternum with light-weight hard armour plates

A. Iwaskiw[1], A. Wickwire[1], M. Vignos[1], C. Howes[1], N. Hahne[1], A. Injeian[1] N. Steiner[1], M. Bevan[1], E. Bar-Kochba[1], E. Mazuchowski[2], M. Clark[3], C. Carneal[1], D. Drewry[1]

[1]*The Johns Hopkins University Applied Physics Laboratory, 11100 Johns Hopkins Road, Laurel, MD 20723, Alexander.iwaskiw@jhuapl.edu*
[2]*Joint Trauma System, 3698 Chambers Pass, Joint Base San Antonio, Fort Sam Houston, TX 78234*
[3]*U.S. Army Combat Capabilities Development Command - Soldier Center / U.S. Special Operations Command, 10 General Greene Avenue, Natick, MA 01760*

Abstract Non-penetrating ballistic events, observed in personal ballistic armour use, are hypothesized to cause blunt injury. These events, termed behind armour blunt trauma (BABT), are not well understood. Early BABT studies involved soft torso armour testing on living goats, which formed the basis of armour performance requirements using a clay backface deformation metric. The lack of understanding of human injury as it is related to non-penetrating ballistic armour performance has contributed to further use of these clay standards for armour design. A more biofidelic human injury model is critical for understanding human injury risk in BABT for evaluation of modern armour systems and optimizing future armour systems.
This study measured BABT, using live ammunition and hard armour, on postmortem human subjects (PMHS) and presents initial observations for a sternum-aligned impact across relevant matched-pair clay deformations. Twelve instrumented PMHS were tested with light-weight hard armour plates along with separate matched-pair clay testing to correlate clay backface deformation to human injury. Combined injuries, coded using the abbreviated injury scale (AIS), ranged from skin damage (AIS $\leq$ 1) to multiple skeletal fractures along with lung lacerations (AIS $\leq$ 5). Further testing is ongoing to produce injury risk prediction models for the injuries seen in this study, and to develop a greater understanding of the influences of biological and experimental variation on injury risk.

1. INTRODUCTION

Modern design of personal armour using advanced materials has led to great improvements in preventing penetrating ballistic injuries [1]. With these personal armour advancements towards reducing armour weight and stopping more powerful rounds, a secondary injury modality, blunt trauma caused by armour deformation, is of increasing concern. These non-penetrating ballistic events, termed behind armour blunt trauma (BABT), while not regularly seen in combat [2] are theorized to be an emerging threat to the warfighter [3]. These BABT injuries are more common in law enforcement environments, due to the prevalence of lighter weight armour systems [4]. There is an ongoing desire in the warfighter community to reduce weight of armour systems while increasing ballistic performance [5]. However, there are concerns with reducing armour weight if it increases the prevalence and severity of BABT injuries to the warfighter community.

Early BABT research focused on soft armour systems. Notably, a series of studies in the 1970's involving soft armour on living goats, formed the basis of the original 44mm clay backface deformation (BFD) standard [6]. This standard's fidelity in assessing performance in newer armour is disputed [7] as it is not based on relevant armour systems or human injury. Studies have stated that there is a lack of human injury data in BABT events with relevant conditions [7, 8]. Continuing to define the relationship of BABT to human injury is critical to allow for continued development of new armour systems.

Classically, postmortem human surrogates (PMHS) have been used for initial evaluations of musculoskeletal injuries. Blunt impact injuries have been studied in automotive safety environments and lower speed blunt ballistic impacts [9-11] and provide a framework for assessing the injury risk. However, due to the uniquely high energy seen in terminal ballistic testing and the viscoelastic nature of the body, prior blunt injury research may fail to appropriately model the injuries hypothesized in BABT. It is also important to note that the relationship between ballistic energy and injury is highly dependent

https://doi.org/10.52202/078352-0017

on the threat and armour pairing. While studies have been conducted evaluating BABT injury [12-15], there exists a need for more injury data in different locations and with different armour threat pairings, as evidenced by current research focus areas [8]. Additionally, these studies have not correlated injuries to the current clay BFD acceptance standard, limiting utility in validating the acceptance standard. It is critically important to identify the scope of potential BABT injuries to inform future armour acceptance criteria and design.

This study introduces an experimental protocol using instrumented PMHS, live ammunition, and light weight hard armour plates to generate BABT impacts to the sternum. Additionally, the injuries observed in this study allow for a better understanding of the potential implications of reducing the non-penetrating armour performance standards for current and future armour systems.

2. METHODS

2.1 Projectile and Armour Combination

The same projectile and armour combination was used for all tests in this study. The projectile chosen is relevant to current operational threats, while velocities were intentionally varied to achieve research goals. The armour was an ultra-high molecular weight polyethylene (UHMWPE) composite multi-curved plate with a Small Arms Protective Insert (SAPI) cut geometry, and it was purposely developed to allow for large clay BFS under specific ballistic test conditions. Each plate was shot once, along the mid-sagittal plane 100mm below the top edge. No backing material or soft armour was used between the hard armour and the impacted subjects in this study as the armour system was designed for the hard armour to be stand-alone.

2.2 Matched-Pair Clay Testing

Knowledge of associated BFS, through matched-pair testing, allows the PMHS aspect of the study to focus on relevant BFS values of interest from armour acceptance standards [6]. Prior to commencing PMHS testing in this study, 60 armour plates were tested to measure clay BFS as a function of round velocity. Testing generally followed the methods described in the National Institute of Justice (NIJ) standard 0101.03 [17]. The clay was scanned before and after each test using a coordinate measurement machine (CMM) FARO (FARO Technologies Lake Mary, Florida) laser scanner to create a point cloud representation of the clay surface. Geomagic Studio software (3D Systems, Rock Hill, South Carolina) was used to transform the point cloud into a surface model and calculate the clay deformation geometry (i.e., BFS).

Projectile velocity measurements were obtained using two sets of Oehler Research model No. 57 infrared screens with Hewlett-Packard (HP) counter chronographs (universal counters, HP model No. 53131A). Velocity was measured 4.6 m from the armour plate and then velocity loss equations were applied specific to the projectile to calculate striking velocity. Projectile velocities were tested across a range of relevant clay BFS, with a typical sample size of 3 for each velocity. The armour was placed on a clay block, with a hand rolled template used to ensure no air gaps behind the curved armour plate. The plates were oriented so that there was approximately 5° obliquity (above horizontal) to the incoming round at the specific shot location, which is consistent with current armour qualification test procedures. All firings were conducted at 7.6 m from the armour sample.

A linear fit of the clay BFS data versus the striking velocity was created. The repeatability was assessed with an r2 value equalling 0.92. The values measured in the clay BFS can be used to help describe the "dose" delivered to the PMHS for use in assessing the relationship between dose and injury for BABT.

2.3 PMHS Demographics

This study investigates the biomechanical response of instrumented PMHS and the associated characteristic injuries incurred by BABT centred over the sternum. The targeted impact location was between the level of the 3rd and 4th ribs, in the midsagittal plane. This study used twelve male, fresh-frozen, non-osteoporotic, full-body PMHS specimens. PMHS were acquired with bilateral

https://doi.org/10.52202/078352-0017

disarticulations at the humerus and femur. All PMHS were acquired under institutional review board exemption approval through Johns Hopkins Medical Institutions. Specimens were selected and acquired based on a controlled range of metrics including age, stature, weight, body mass index (BMI) and lumbar bone mineral density (BMD) based on Dual Energy X-ray Absorptiometry (DEXA), which are shown later with injury results in Table 2. Additionally, specimens with prior trauma or severe thoracic diseases requiring invasive surgical interventions were restricted from this study.
Once received, high-resolution computed tomography (CT) scans (slice thickness of 0.625 mm) were acquired for specimens at the Johns Hopkins University Applied Physics Laboratory (JHUAPL) to ensure no abnormalities or signs of trauma were apparent that could influence interpretation of injury. Specimens were stored at −20 ◦C until being thawed at 1.6 ◦C 6 days prior to testing for instrumentation and test preparation.

2.4 PMHS Instrumentation

Specimens were instrumented with high-rate biomechanical sensors in order to gain an understanding of the mechanical event and to measure potential mechanical correlates to injury. It is important to note that the instrumentation methodology was determined based on a desire to not affect injury outcomes, so key structures were left intact and minimally invasive techniques were used. While not a focus of this paper, it is important to introduce the sensors to help understand future analyses.

Instrumentation was placed on the surrounding torso skeletal system, and in key organ systems. Specific information, including location, type, and quantity of sensors are shown in Table 1. Generally, the instrumentation was grouped by skeletal motion, skeletal strain, skeletal acoustic emissions, critical organ pressure, and surface contact.

Table 1. Specimen instrumentation

Sensor Description	Location	Type	#
Rib strain	Anterior ribs 2-7, Posterior ribs 4-9	Single axis strain gauge (Kyowa KFWB-2-350)	24
Rib/Sternum Acoustic Emission	Lateral ribs 2-7, Superior manubrium	Acoustic emission sensor (Mistras Nano30)	14
Lung pressure	Left and right bronchi	Pressure transducer (Kulite XCL-100- 100A)	4
Liver pressure	Medial and lateral lobe; parenchyma	Pressure transducer (Kulite XCL-100- 100A)	4
Spleen pressure	Mid-parenchyma	Pressure transducer (Kulite XCL-100- 100A)	2
Aortic arch pressure	Aortic arch	Pressure transducer (Kulite XCL-100- 100A)	2
Left ventricle pressure	Lent ventricle	Pressure transducer (Kulite XCL-100- 100A)	2
Sternum acceleration	Superior manubrium and xiphoid (internal face)	Single-axis accelerometer (Endevco 727)	2
Spine acceleration	Co-aligned spinal level to impact location (varies)	Single-axis accelerometer (Endevco 727)	1
Surface force	On surface directly under impact, 38mm superior, left, inferior, right of impact location	Contact sensor (TekScan flexiforce 301)	5

Along with instrumentation, the specimens were outfitted with catheters and intubation equipment to perfuse the cardiovascular system and insufflate the lungs, respectively. Foley catheters were placed through the carotid arteries to the aortic arch and left ventricle of the heart, with the purpose of blocking flow out of this region of the cardiovascular system. Additionally, a Foley catheter was placed in the femoral artery. This catheter extended superior to the renal branching which allowed for isolation of the descending aorta, the aortic arch and the left ventricle. Contrast fluid was introduced to the isolated region to ensure proper installation, verified by CT. Active static pressure of 80 mmHg was introduced to the isolated heart region during the test to simulate normal cardiovascular pressure.

An intubation tube was placed through a tracheotomy used for sensor install, which was fitted to a down-regulated air compressor. Approximately 7 kPa of positive pressure was used to insufflate the lungs during the test. CT was used to ensure the lungs were fully insufflated and contacting the interior

https://doi.org/10.52202/078352-0017

surface of the anterior plural wall. A post-instrumentation, insufflated CT was taken to capture final sensor location, perfusion and insufflation.

https://doi.org/10.52202/078352-0017

2.5 PMHS BABT Experimental Setup

After instrumentation, the PMHS were transported to a NIJ certified commercial ballistic test lab. The specimens were placed on a custom mounting rig, resembling a table, and rotated upright. The specimens were strapped to the mounting rig using nylon straps around the forehead, shoulders, waist, and legs. The PMHS were supported by a seat, and the rig provided a rigid boundary condition at the back. The impact location of the specimen was in the middle of the sternum in the mid sagittal plane, specifically over the sternum between the levels of the 3rd and 4th ribs. The rig was adjusted, after insufflating the lungs, so that the impact location on the specimen was aligned with the ballistic target, and small adjustments were made to ensure the specimen was upright and symmetrical, simulating a front-on shot to the mid sternum (Figure 1).

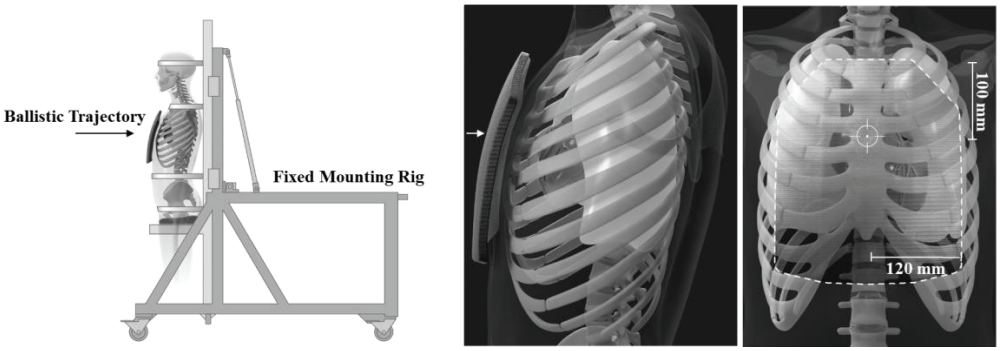

Figure 1. (Left) PMHS experimental setup. (Right) Lateral and frontal specimen and armour impact location

The armour used in the study was aligned with the shot location on the specimen using a custom carrier with holes centred on the impact location cut out to ensure no influence of the carrier to the BABT loading. The standoff of the plate, from the rear surface of the plate to the external surface of the skin, was measured using a FARO CMM. This was achieved by comparing the impact location on the PMHS before donning the armour to the impact location on the impact face of the armour after donning and subtracting out the armour thickness. Armour was donned to provide a "normal fit", which compressed parts of the PMHS but resulted in a sizable air gap between the armour and specimen at the impact location due to the curvature of the armour and curvature of the chest between the pectoral muscles. The armour standoff and obliquity was not controlled, but it was measured, spanning 3-25 mm and 5-13° above horizontal, respectively. Pretest x-rays and photos were taken of the perfused and insufflated PMHS directly before the ballistic impact to ensure proper anatomical targeting and measure upright/in situ sensor locations, shown in Figure 2.

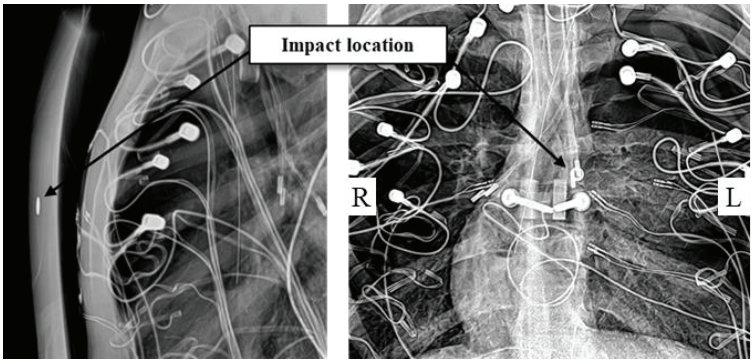

https://doi.org/10.52202/078352-0017

Figure 2. Characteristic (APL 11) specimen planar x-ray views of the sternum laterally (left) and anteroposterior of the sternum and spine (right) prior to impact.

The PMHS were then subjected to BABT loading by a single live-fire ballistic projectile across a range of relevant velocities and associated backface deformations. Projectile velocity measurements were obtained similarly to the clay matched-pair testing. A high-rate data acquisition system (Dewetron Inc., East Greenwich, RI, model DEWE-801) was used to record PMHS sensor data at 1 MHz sampling rate. Acoustic emissions sensor data was collected using a PicoScope 5000 high-rate data acquisition system (Pico Technology, Cambridgeshire, UK) at a 4.8 MHz sampling rate to accommodate higher frequencies of interest. Additionally, two high-speed camera systems (Vision Research Inc., Wayne, NJ, model Phantom v711) recorded the ballistic event at a rate of over 22,000 frames per second from both a lateral and oblique view of the specimen. All electronics systems were simultaneously triggered with the signal disruption of a frangible breakscreen by the incoming round. All instrumentation signals, accept for the acoustic emission data, were subject to a 300-kHz anti-alias filter.

2.6 Post-Test Evaluation and Forensic Analysis

Directly after the BABT impact, post-test x-rays and photos were taken, making sure not to disrupt any armour placement or insufflation. The specimens were carefully returned to a supine position and then transported back to JHUAPL for post-test CTs. Post-test CT scans were taken with insufflated lungs with armour on, armour off, and skeletal instrumentation removed. The specimen CTs were reviewed by a board-certified forensic pathologist who subsequently led an anatomical dissection of the PMHS. A detailed report, with associated pictures, for each PMHS was created to characterize and preliminarily assess severity of any injuries sustained as a result of the BABT.

3. RESULTS

3.1 Injuries

Injuries were observed, depending on their severity, in post-test x-rays, CT, and anatomical dissection, highlighted with representative images from a severe case in Figure 3. Typical post-test x-rays showed the residual armour deformation and underlying anatomical defects. CT scans were able to further identify the extent of the injury, where single slice views and maximum intensity projection images showed particularly compelling evidence of injury. Finally, an anatomical dissection was conducted to concretely evaluate the characteristics and severity of the injuries identified in the medical imaging. During this step, skeletal components were physically manipulated to assess fracture, the lungs were inflated after opening the pleura to identify lacerations, and organs were removed sequentially for further analysis. Autopsy notes were taken and integrated into injury scoring analysis using the abbreviated injury scale (AIS) [18]. AIS provides a relationship between a particular injury and probability of lethality. Associated injuries ranged from skin damage (AIS $\leq$ 1) to multiple skeletal fractures along with lung lacerations (AIS $\leq$ 5).

https://doi.org/10.52202/078352-0017

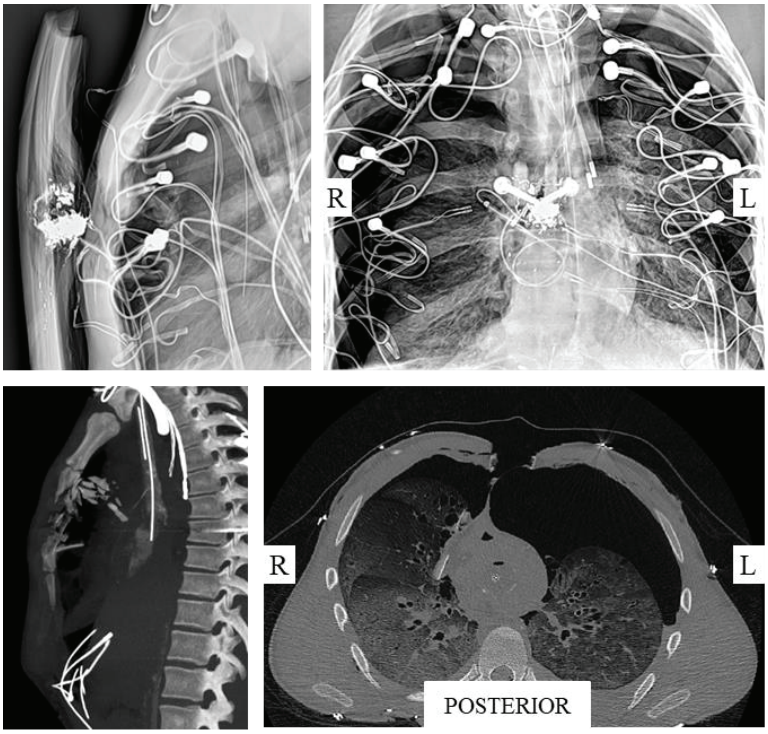

Figure 3. Characteristic (APL 11) specimen medical images after impact; (Top Left) lateral planar x-ray view of the sternum with armour on, (Top Right) anteroposterior planar x-ray of the sternum and spine with armour on, (Bottom Left) maximum intensity projection image of sternum damage in the sagittal plane with armour removed, (Bottom Right) axial CT slice at impact level with armour removed.

In order to quantify the most consequential injury, maximum abbreviated injury scale (MAIS) can be used to compare cases. An alternative way to assess the severity of a complex injury is to use the New Injury Severity Score (NISS) injury model [19]. The NISS is calculated from AIS scores and is the sum of the squares of most severe AIS coded injuries, regardless of body region. These injury outcomes can be found in Table 2. Individual injury codes can be found in Appendix 1.

Table 2. Specimen summary and injury results

APL Identifier	Age	Cause of Death	Stature (cm)	Full Body Weight (kg)	BMI (kg/m^3)	DEXA (T-Score)	MAIS	NISS
APL 01	60	Acute respiratory failure	175	71	23.03	-0.3	3	14
APL 02	64	Lung cancer	180	79	24.27	-0.4	3	17
APL 03	65	Glioblastoma multiforme	173	93	31.17	-0.8	3	14
APL 04	44	Glioblastoma multiforme	175	80	26.14	-0.5	1	2
APL 05	52	Cardiac arrest	170	67	23.02	0.5	3	17
APL 06	63	Metastatic brain cancer	178	89	28.26	0.7	3	14
APL 07	55	Sepsis	183	73	24.63	2.2	3	14
APL 08	57	Deep Vein Thrombosis	183	99	29.6	-0.5	2	9
APL 09	25	Complications: anoxic-ischemic encephalopathy	178	64	20.37	0.4	5	43
APL 10	20	Asphyxiation	178	69	21.8	-0.5	5	50
APL 11	63	Lewy Body Disease	183	100	29.8	-0.5	5	50
APL 12	62	Neoplasm of the Pancreas	178	72	22.7	0.7	5	66

https://doi.org/10.52202/078352-0017

4. DISCUSSION

4.1 PMHS Injury Outcome

Although the study is ongoing, an early identification of characteristic injuries can aid future armour design and policy. It is important to note that a majority of the clay BFS dose values used in this study are at or above the most widely adopted 44mm standard.

Thus far, four main injury presentations have emerged. The first, and least severe injury type, is a skin and soft tissue only injury. APL04 is the only result that falls into this injury outcome grouping. The AIS and NISS scores for this grouping are 1 and 2 respectively, and this outcome represents a minor injury. Future assessments planned for this study, leveraging medical experts, can further help characterize the likely clinical outcome for a living individual and the medical treatment needed for effective combat casualty care response.

The second grouping of injuries can be broadly characterized as skin and soft tissue and skeletal injuries. Five cases (APL 01, APL 03, APL 06, APL 07, APL 08) are categorized to this grouping. These cases present as skin and soft tissue injuries, crushing local fractures of the sternum (behind the impact location), and anterior fractures/separations of the ribs approximately 2-8 cm from the midline. MAIS spanning 2 to 3, and NISS spanning 9 to 14 are seen in this group. The singular MAIS 2 case injury outcome in this group, APL 08, is nearly indistinguishable from MAIS 3 of this group. The scoring distinction is that APL 08 resulted in less than 3 rib fractures, reducing its rib fracture AIS score from 3 to 2. Although in the absence of functional outcomes, the observed outcomes are assigned a serious outcome level.

The third grouping includes the same skin and soft tissue and skeletal injuries seen in the serious cases with the addition of communication with the anterior mediastinum, which could result in hemo- and pneumo- mediastinum (APL 02, APL 05). While this group does not have a higher MAIS than the serious cases, the additional clinical complication of another severe thoracic injury results in a less promising clinical outcome due to an increased risk of infection. The MAIS and NISS in this grouping are 3 and 17, respectively, with an assigned outcome level of severe.

grouping, these cases (APL 09, APL 10, APL 11, APL 12) share injuries such as skin damage, skeletal fracture, and communication with the anterior mediastinum. What differentiates these cases is the presence of damage of the underlying thoracic tissue, some suggesting pneumothorax. Accordingly, these four cases are assigned an outcome level of critical. Pneumothorax would require rapid medical intervention and is life threatening. The presence of these lung lacerations were identified through post-test x-ray and CT, where previously insufflated lungs were collapsed, and then confirmed in the anatomical dissection. Other injuries seen were flail chest rib fractures (3 adjacent ribs with 2 or more fractures), communication with the pleural cavity, laceration of the pericardial sac, and discoloration on the heart suggesting the likelihood of myocardial contusion in a living individual. These critical injuries suggest varied injuries of the thoracic organs can occur due to BFD. It was further observed that the natural positioning of key organs (e.g. anterior aspect of lung lobes positioned across mid sagittal plane directly under the impact location, mediastinum and heart directly under impact location, etc.) can influence which organs can be injured and subsequent severity. Not only does this sensitivity have implications for developing a validated human-based injury prediction model, but also for the operational medical community, as these injuries represent new challenges to combat casualty care.

The grouping of these injuries represents a pathway of likely injury outcomes. The least severe injury grouping consists of superficial injuries, and with incrementing case severity, more damage is seen deeper towards the centre of the body. However, in no way do the authors believe these categorical injury outcomes are linearly related to the dose, thusly requiring more data in each injury grouping to identify the complete injury risk spectrum [19]. The injuries seen in this study are very local and are similar to injuries seen in other similar mediastinal blunt trauma studies [11, 13], although some of the critical injuries seen in this study have not been observed before.

https://doi.org/10.52202/078352-0017

4.2 Study Limitations

This study has highlighted that, for the tested conditions, none are absent of injury, and injury severities vary greatly. It is important, however, to appropriately caveat the data as preliminary with ongoing efforts to further understand the relationship between dose and injury outcome, when dose is defined by the current clay test methodology. Additionally, due to the limitations in this model, further work must be done to understand the usability of this data in future injury risk prediction.

First, it is well known that mechanical properties of previously frozen PMHS tissue (especially soft and connective tissue) can vary from living tissue [20] and are absent of critical physiological responses. As a result, there is limited understanding of how valid soft tissue injuries are in PMHS [21]. It is important to understand the changes in tissue material properties and quality when interpreting organ injury. Non-living organs cannot accurately model lower severity organ injuries such as contusions, so living animal models may be a better model for these minor injuries. The authors believe, however, that the types of organ injuries that were observed (lacerations) and the fact that the organs of interest were properly inflated/perfused results in appropriate suggestions of potential injuries in a living human. Additionally, PMHS demographics, due to factors such as age and pathology, have been observed to contribute to a greater injury risk [22]. Ultimately, the fidelity provided by the near perfect geometrical model of a PMHS is critical in early understanding of injuries. The authors did adhere to a strict acquisition protocol, restricting age and limiting specimens with any signs of bone degeneration or disease.

Another limitation to this study is the use of a single threat/armour pairing in a limited range of dose conditions. It is very important to understand that extrapolation of this data to higher or lower doses or to other classes of armour and threats may not apply without verifying with further testing. For example, with the absence of a clothing or soft armour, the results in this study do not explain the role of soft armour in preventing BABT injuries, so further exploration is required for armour systems that include soft armour. Additionally, more information characterizing the specific contribution of the armour/threat pairing to BABT loading to the body should be generated before using this injury risk information on other cases. Other studies using mechanical surrogates can contribute greatly to the understanding of the conditions that lead to BABT injury [23, 24].

Another limitation of this study is the evaluation of a single impact location. The severe injuries seen in this study are dependent on the placement of organs with respect to the impact location. Further studies should explore key organ location and the distance/depth from potential BABT loading as well as the structural composition of the skeleton at that area [25].

Armour donning is thought to play a large role in BABT injury as “normal fit” resulted in anywhere from 3-25 mm of standoff in this study. Additionally, tissue composition and chest shape/anatomy varies within the population and could greatly affect the engagement of the armour BFD and the underlying anatomy. The authors are investigating the effect of standoff and flesh thickness, and believe that further studies should characterize the “normal fit” in military populations so that the injury risk developed in this study can be appropriately scaled to military population fit and local anatomical conditions.

5. CONCLUSION

This paper introduces an experimental methodology and initial injury results for live-fire non-penetrating ballistic impacts on instrumented PMHS. Early observations in tests show injuries ranging from minor (skin and soft tissue laceration) to critical (skin and soft tissue laceration, multiple complex skeletal fractures, lacerated lungs) that can be categorized into four distinct notional injury groupings: minor, serious, severe, and critical. The resulting injuries were generally localized to the region of armour deformation. While injury results have much value, it is important to understand that they are closely related with the conditions of this test series, and should not be extrapolated to other impact locations or armour/threat pairings without further testing. It is critical to the future use of this data for additional work to be done to understand emerging hypothesized contributors to injury risk, such as armour fit, anatomical/geometric variation, and armour type. However, the authors do believe that severe injury outcomes, as a result of BABT, are possible and that steps should be taken to ensure that future armour systems appropriately optimize the trade-offs between BABT protection and other design factors.

https://doi.org/10.52202/078352-0017

Acknowledgments

The authors would like to express their appreciation to the U.S. Special Operations Command and the US Army Combat Capabilities Development Command Soldier Center (CCDC Soldier Center) for funding this work under Contract No. is H92222-15-D-0004.

References

[1] Prat, et al., Contemporary body armor: technical data, injuries, and limits, European journal of trauma and emergency surgery 38.2 (2012); pp. 95-105.

[2] Carr, et al., Is behind armour blunt trauma a real threat to users of body armour? A systematic review, Journal of the Royal Army Medical Corps 162.1 (2016); pp. 8-11.

[3] Carroll, et al., A new nonpenetrating ballistic injury, Annals of surgery 188.6 (1978); pp. 753.

[4] Cannon L, Behind armor blunt trauma - an emerging problem, J R Army Med Corps. 2001; pp. 147:87–96.

[5] Bhatnagar, Lightweight ballistic composites: military and law-enforcement applications, Woodhead Publishing (2016).

[6] Montanarelli, et al., Protective garments for public officials. No. LWL-CR-30B73. Army Land Warfare Lab Aberdeen Proving Ground MD (1973).

[7] Hanlon, et al., Origin of the 44-mm behind-armor blunt trauma standard, Military Medicine 177.3 (2012); pp. 333-339.

[8] National Research Council, Testing of body armor materials: Phase III, National Academies Press, (2012).

[9] Kroell, et al., Impact tolerance and response of the human thorax II, SAE Transactions (1974); pp. 3724-3762.

[10] Viano,et al., A viscous tolerance criterion for soft tissue injury assessment, Journal of Biomechanics 21.5 (1988); pp. 387-399

[11] Bir, et al., Design and injury assessment criteria for blunt ballistic impacts, *Journal of Trauma and Acute Care Surgery* 57.6 (2004); pp. 1218-1224.

[12] Raymond, et al., Tolerance of the skull to blunt ballistic temporo-parietal impact, Journal of biomechanics 42.15 (2009); pp. 2479-2485.

[13] Bass, et al., Injury risk in behind armor blunt thoracic trauma, International journal of occupational safety and ergonomics 12.4 (2006); pp. 429-442.

[14] Rafaels, et al, Injuries of the head from backface deformation of ballistic protective helmets under ballistic impact, J. Forensic Sci., 60 (2015); pp. 219-225

[15] Mirzeabassov, et al., Further investigation of modelling for bullet-proof vests. In: Proceedings from the 5th Personal Armor Safety Symposium. Colchester, UK: International Personal Armour Committee (2000); pp. 211–34.

[17] Standard, N. I. J., 0101.06, Ballistic Resistance of Body Armor (2008); pp. 1-89.

[18] Gennarelli.,et al., AIS 2005, Association for the Advancement of Automotive Medicine, Barrington, IL (2005)

[19] Stevenson, et al., An overview of the injury severity score and the new injury severity score, Injury Prevention 7.1 (2001); pp. 10-13

[20] Hohmann, et al., The mechanical properties of fresh versus fresh/frozen and preserved (Thiel and Formalin) long head of biceps tendons: A cadaveric investigation, Annals of Anatomy-Anatomischer Anzeiger 221 (2019); pp. 186-191

[21] Nahum, et al., eds., Accidental injury: biomechanics and prevention, Springer Science & Business Media (2012).

[22] Laituri, et al. Derivation and evaluation of a provisional, age-dependent, AIS3+ thoracic risk curve for belted adults in frontal impacts. No. 2005-01-0297. SAE Technical Paper, 2005.

[23] Bevan. et al., Investigation of Armor and Round Effects on Water-Based Armor Assessment System Measurements, Personal Armour Systems Symposium 2016, Amsterdam, NL, (2016).

https://doi.org/10.52202/078352-0017

[24] Merkle A., et al., Assessing behind armor blunt trauma (BABT) under NIJ standard-0101.04 conditions using human torso models, Journal of Trauma and Acute Care Surgery 64.6 (2008); pp. 1555-1561

[25] Carneal C., et al., A Computational Pipeline Enabling the Generation of Multi-Organ Statistical Atlases for Improved Human Model Development, Military Health System Research Symp Kissimmee, FL (2016).

Appendix I

Table 1. Complete injury coding data

APL Identifier	AIS Coding of injury observed	
APL01	3 [450203.3]	Rib Cage; fracture(s) w/o flail; any location unilateral or bilateral ≥3
	2 [450804.2]	Sternum; fracture
	1 [410602.1], 1 [410202.1]	Skin; laceration, Skin; abrasion
APL02	3 [450203.3]	Rib Cage; fracture(s) w/o flail; any location unilateral or bilateral ≥3
	2 [442208.2]	Thoracic injury; Hemomediastinum
	2 [442209.2]	Thoracic injury; Pneumomediastinum
	2 [450804.2]	Sternum; fracture
	1 [410602.1], 1 [410202.1]	Skin; laceration, Skin; abrasion
APL03	3 [450203.3]	Rib Cage; fracture(s) w/o flail; any location unilateral or bilateral ≥3
	2 [450804.2]	Sternum; fracture
	1 [410602.1], 1 [410202.1]	Skin; laceration, Skin; abrasion
APL04	1 [410602.1], 1 [410202.1]	Skin; laceration, Skin; abrasion
APL05	3 [450203.3]	Rib Cage; fracture(s) w/o flail; any location unilateral or bilateral ≥3
	2 [442208.2]	Thoracic injury; Hemomediastinum
	2 [442209.2]	Thoracic injury; Pneumomediastinum
	2 [450804.2]	Sternum; fracture
	1 [410602.1], 1 [410202.1]	Skin; laceration, Skin; abrasion
APL 06	3 [450203.3]	Rib Cage; fracture(s) w/o flail; any location unilateral or bilateral ≥3
	2 [450804.2]	Sternum; fracture
	1 [410602.1], 1 [410202.1]	Skin; laceration, Skin; abrasion
APL 07	3 [450203.3]	Rib Cage; fracture(s) w/o flail; any location unilateral or bilateral ≥3
	2 [450804.2]	Sternum; fracture
	1 [410602.1], 1 [410202.1]	Skin; laceration, Skin; abrasion
APL 08	2 [450202.2]	Rib Cage; fracture(s) w/o flail; any location unilateral or bilateral <3
	2 [450804.2]	Sternum; fracture
	1 [410602.1], 1 [410202.1]	Skin; laceration, Skin; abrasion
APL 09	5 [442204.5]	Left chest, pneumothorax
	3 [450203.3]	Rib Cage; fractures w/o flail ≥3
	3 [441431.3]	Left lung, laceration
	2 [450804.2]	Sternum; fracture
	1 [410602.1], 1 [410202.1]	Skin; laceration, Skin; abrasion
APL 10	5 [442204.5]	Right chest, pneumothorax
	4 [415000.4]	Open ('sucking') chest wound
	3 [450203.3]	Rib Cage; fractures w/o flail ≥3
	3 [441431.3]	Right lung, laceration
	2 [450804.2]	Sternum; fracture
	1 [410602.1], 1 [410202.1]	Skin; laceration, Skin; abrasion
APL 11	5 [442204.5]	Left chest, pneumothorax
	4 [415000.4]	Open (sucking) chest wound
	3 [450212.3]	Rib Cage; fractures with flail, 3-5 ribs
	2 [450202.2]	Rib Cage; fractures w/o flail; any location unilat or bilat, 2 ribs
	3 [441431.3]	Left lung, laceration
	2 [450804.2]	Sternum; fracture
	1 [441004.1]	Heart; contusion
	1 [410602.1], 1 [410202.1]	Skin; laceration, Skin; abrasion
APL 12	5 [442204.5]	Left chest, pneumothorax
	5 [450214.5]	Bilateral flail chest
	4 [415000.4]	Open ('sucking') chest wound
	3 [441010.3]	Heart; laceration
	2 [441602.2]	Pericardium, laceration
	2 [450804.2]	Sternum; fracture
	1 [410602.1], 1 [410202.1]	Skin; laceration, Skin; abrasion

https://doi.org/10.52202/078352-0017